Evaluation of wind tunnel wall interference using homogeneous and measured boundary conditions

Mihaela BURGHIU*

*Corresponding author
*INCAS – National Institute for Aerospace Research "Elie Carafoli",
B-dul Iuliu Maniu 220, Bucharest 061126, Romania,
manea.mihaela@incas.ro

DOI: 10.13111/2066-8201.2023.15.4.5

Received: 23 October 2023/ Accepted: 03 November 2023/ Published: December 2023

Abstract: *The experimental results obtained in a wind tunnel must be subjected to a correction process which aims to eliminate the influence of the limited dimensions of the flow field around the model. This is necessary because the results must be independent of the characteristics of the laboratory where they were obtained, in order to ensure the quality of the parameters.The wall corrections are applied to the global quantities that characterize the undisturbed flow, such as the Mach number or the dynamic pressure, but they are also applied to the quantities related to the model, namely the global aerodynamic coefficients.Consequently the corrections will be applied to the global quantities of the undisturbed flow and therefore they will be transmitted to the aerodynamic quantities related to the model.*

Key Words: *Wind tunnel, wall interference, ventilated wall, potential flow theory*

1. INTRODUCTION

Typically, wall corrections are classified into primary corrections, which are applied to the Mach number and the angle of attack, and higher-order corrections.

Blockage corrections occur as a result of the axial component of the induced velocity. Their purpose is to compensate for the volume of the model and its wake, the blockage being the result of the interaction between the physical volume of the model and the walls of the test section. Blockage corrections are defined by using the blockage factor, ε, which is the ratio between the axial component of the velocity due to the presence of the walls and the reference flow velocity [1]. The blockage factor is applied as a correction to the dynamic pressure and to the Mach number.

The magnitude of the corrections is influenced by the type of walls. In the case of solid walls, these corrections are usually higher and have a positive value, unlike the case of ventilated walls, when their value is smaller and also have a negative sign.

$$\varepsilon = \frac{u_W}{U} \tag{1}$$

Lift interference corrections are due to the vertical component of the induced velocity. They influence the angle of attack of the model. If the lift coefficient is positive, this correction has a positive value in solid walls, and a negative value in perforated walls.

$$\Delta\alpha = \frac{w_W}{U} \tag{2}$$

Higher order corrections occur because the primary interference is not constant between different regions of the model. Pitching moment corrections can be computed as a function of the variation of the angle of attack along the span or chord. Buoyancy correction can be computed as the variation of the blockage factor along the fuselage.

To account for the behaviour of the ventilated wall it is necessary to properly determine the boundary conditions. An useful simplification of the boundary conditions consisted in considering the ventilated wall as homogeneous, the solid and free portions not being treated separately, but as an equivalent permeable surface.

In [2] the boundary condition for perforated walls was generalized and a panel method was developed to determine the lift interference:

$$c_1\varphi + c_2\frac{\partial\varphi}{\partial x} + c_3\frac{\partial\varphi}{\partial n} + c_4\frac{\partial^2\varphi}{\partial x\partial n} = 0 \tag{3}$$

Table 1: c_1 ,…, c_4 coefficients

Type of boundary condition	c_1	c_2	c_3	c_4
Solid walls	0	0	1	0
Open jet	0	1	0	0
Perforated walls	0	1	$\frac{1}{P}$	0

Here P represents the porosity parameter, which characterizes the behavior of the ventilated walls during the experiments and must be determined for each wind tunnel.

The importance of measuring boundary conditions has been recognized for a long time, due to the fact that by using them the obtained corrections give a more accurately description of the phenomena during the experiments.

The one-variable method is the most popular method for evaluating wall interference using pressure distributions measured on the wall of the test section. This method is only valid for subsonic, irrotational flows. It is assumed that the potential near the walls is governed by the linear Prandtl-Glauert equation.

$$\beta^2\frac{\partial^2\varphi}{\partial x^2} + \frac{\partial^2\varphi}{\partial y^2} + \frac{\partial^2\varphi}{\partial z^2} = 0 \tag{4}$$

The potential consists of two parts, namely the potential due to the flow around the model and the potential due to the interference of the walls.

$$\varphi = \varphi_M + \varphi_W \tag{5}$$

In the above equation, φ_M can be interpreted as the potential generated by the model if the same forces would act on it in free flow and φ_W is the interference potential induced by the walls [3].

The difference between the theoretical approach and the use of the boundary conditions obtained experimentally, consists in replacing the idealized boundary condition by the measured one.

$$\frac{\partial \varphi}{\partial x} = u \tag{6}$$

$$u = \frac{U - U_\infty}{U_\infty} \tag{7}$$

u is the measured component of the perturbation velocity.

2. WALL CORRECTIONS COMPUTATION USING HOMOGENEOUS BOUNDARY CONDITIONS

As previously mentioned, the general definition of wall corrections is the difference between the flow around a body in infinite current and the flow around the same body in a current bounded by wind tunnel walls.

The lift interference is caused by the change produced by the walls in the circulation generated by the model in the wind tunnel. A first consequence of the lift interference is represented by the alteration of the flow near the model which directly affects the angle of attack. The second consequence is the curvature of the air flow direction.

Blockage corrections are applied to the flow parameters in the test section, mainly to the dynamic pressure, which is then used to determine the aerodynamic coefficients.

Blockage corrections fall into two categories, namely solid blockage corrections due to model-induced axial velocity and wake blockage corrections due to wake-induced axial velocity.

The blockage in the wind tunnel influences the velocity of the free stream, therefore it is necessary to correct the reference quantities of the flow: velocity, Mach number, dynamic pressure, static pressure, static temperature, density and Reynolds number. For a small correction factor and $\gamma = 1.4$, the linearized corrections of these reference quantities are [4]:

$$U_\infty = U_{CE}(1 + \varepsilon) \tag{8}$$

$$M_\infty = M_{CE} \cdot [1 + (1 + 0.2M_{CE}^2)\varepsilon] \tag{9}$$

$$q_\infty = q_{CE} \cdot [1 + (2 - M_{CE}^2)\varepsilon] \tag{10}$$

$$p_\infty = p_{CE} \cdot [1 - 1.4M_{CE}^2\varepsilon] \tag{11}$$

$$T_\infty = T_{CE} \cdot [1 - 0.4M_{CE}^2\varepsilon] \tag{12}$$

$$\rho_\infty = \rho_{CE} \cdot [1 - M_{CE}^2\varepsilon] \tag{13}$$

$$Re_\infty = Re_{CE} \cdot [1 + (1 - 0.7M_{CE}^2)\varepsilon] \tag{14}$$

By relating the global aerodynamic forces and moments, measured on the model in the experimental chamber, to the corrected value of the dynamic pressure, the corresponding dimensionless coefficients, corrected with the influence of the blockage, will be obtained by applying:

$$C_{F_c} = \frac{F}{q_c} = \frac{F}{q}\frac{1}{[1 + (2 - M_{CE}^2)\varepsilon]} \tag{15}$$

Classical corrections have been developed for all types of experimental sections: solid walls, open-jet, perforated walls and slotted walls. The classical theory of wall corrections is

based on the assumption of a linearized potential flow without shock waves or flow separations. Thus, the velocity field at any point can be defined as [5]:

$$\vec{U}(x,y,z) = \nabla\Phi(x,y,z) \tag{16}$$

Assuming that the principle of linear superposition is valid, the potential Φ can be expressed as the superposition of the flow potential, the model potential, φ_M, and the wall interference potential, φ_W.

A panel method based on the potential flow theory was developed in order to estimate the wall corrections obtained in this paper The homogeneous boundary conditions were determined using a porosity parameter characteristic for the INCAS perforated wall test section, while the measured boundary conditions were determined by means of the pressure distributions obtained on the walls of the experimental chamber.

Compressibility was taken into account by using the Prandtl-Glauert compressibility factor.

The test section walls were divided into rectangular elements, each of these elements being represented by a distribution of sources with constant intensity along the element.

$$\varphi_W = \sum_{i=1}^{N} \varphi_i^* \sigma_i' \tag{17}$$

If we consider a certain rectangular element, then the potential, φ^* in a point with (x,y,z) coordintes is [2]:

$$\varphi^* = -\int_{\xi_1}^{\xi_2}\int_{\eta_1}^{\eta_2} \frac{(\xi-\xi_1)d\xi d\eta}{\sqrt{(x-\xi)^2+(y-\eta)^2+(z-\zeta_1)^2}} - \int_{\xi_2}^{\xi_L}\int_{\eta_1}^{\eta_2} \frac{(\xi_2-\xi_1)d\xi d\eta}{\sqrt{(x-\xi)^2+(y-\eta)^2+(z-\zeta_1)^2}} \tag{18}$$

The boundary conditions satisfied at the centroid of each element can be written for all four walls as follows:

$$\frac{\partial\varphi}{\partial x} - \frac{1}{P}\frac{\partial\varphi}{\partial z} = 0 \tag{19}$$

$$\frac{\partial\varphi}{\partial x} + \frac{1}{P}\frac{\partial\varphi}{\partial z} = 0 \tag{20}$$

for the top and bottom walls, and

$$\frac{\partial\varphi}{\partial x} - \frac{1}{P}\frac{\partial\varphi}{\partial y} = 0 \tag{21}$$

$$\frac{\partial\varphi}{\partial x} + \frac{1}{P}\frac{\partial\varphi}{\partial y} = 0 \tag{22}$$

for the side walls.

The model was represented by lifting lines located at ¼ of the chord and the lift distribution is assumed to be elliptical. Therefore, the model can be represented by a distribution of vortices described by the potentials [6]:

$$\varphi_{M_j} = \frac{\gamma_j}{4\pi}\frac{z}{y^2+z^2}\left(1+\frac{x}{\sqrt{x^2+y^2+z^2}}\right) \tag{23}$$

The fuselage of the model is represented by using three-dimensional doublets, distributed along the central axis.

$$\varphi_M^S = \frac{d}{4\pi}\frac{x}{(x^2+y^2+z^2)^{3/2}} \tag{24}$$

$$d = UV \tag{25}$$

The wake effect was approximated by using a point source.

$$\varphi_M^D = \frac{-\sigma}{4\pi}\frac{1}{(x^2+y^2+z^2)^{1/2}} \tag{26}$$

$$\sigma = \frac{1}{2}SC_D \tag{27}$$

For the calculation of the source intensities slopes, necessary to satisfy the boundary conditions, a matrix equation must be solved for the values of σ_j', used later in the determination of the interference potential due to the walls.

2.1 Incompressible flow

The lift correction is calculated using the panel method described in previous chapter, starting from the potential flow assumption.

The walls of the experimental chamber were divided into 416 panels, and the lifting effect of the wings was represented by a distribution of 20 vortices.

The correction factor, δ_0, was calculated at three locations namely the tip of the wing, the center of the lift distribution and the wing root.

The obtained results are compared with some results in the existing literature, both to observe the character of the perforated walls, and to validate them.

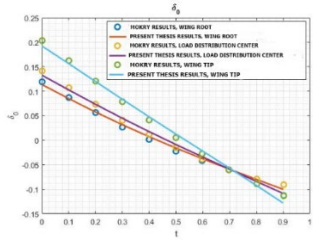

Fig. 1: Lift interference correction factor represented in all three locations

The solid blockage correction factor was determined using the panel method described previously. The number of rectangular elements into which the experimental room was divided is also the same as for the lift interference.

In order to perform the comparison with the results in the literature, the model was represented by a single three-dimensional doublet, placed in the center of the test section at $x = 0, y = 0, z = 0$.

The intensity of the three-dimensional doublet was taken to be equal to 1, and the width and height of the test section were both taken to be equal to 1.

The results are compared with those in [7], where the same model representation was used.

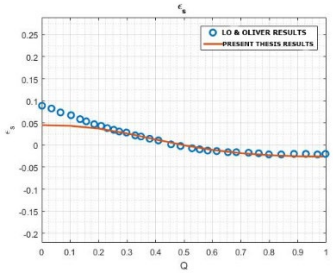

Fig. 2: Solid blockage interference factor

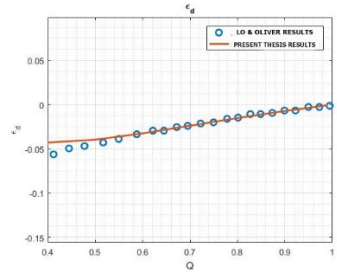

Fig. 3: Wake blockage interference factor

Wake blockage is caused by the finite size of the wake left by the model and is similar to solid blockage.

For the computation of the results presented below, the wake was represented by means of a source, having the intensity equal to 1 and placed in the center of the test section. The results were also compared with those in [7].

2.2 Compressible flow

The equations describing the compressible flow are non-linear and do not have a general solution, their evaluation being possible with the help of numerical methods. Their linearization represented a practical solution, as it did not involve the use of significant computational resources. However, the solutions thus obtained are considered to be only approximate [8].

For solid walls, the corrections were computed by following the procedure presented in the previous subsection and imposing the appropriate boundary conditions. The compressibility effect has also been added [9].

The results presented in this subsection were obtained for the ONERA M4R model, in the INCAS trisonic wind tunnel, in the solid walls test section. The test section was represented using 1664 rectangular elements, the effect of the wing was represented using a distribution of 20 vortices, the effect of the fuselage was represented using 10 three-dimensional doublets, and the effect of the trail using a point source [10].

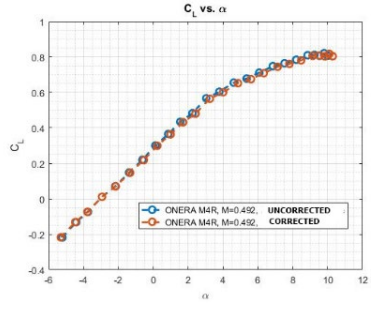

Fig. 4: Uncorrected lift coefficient vs. corrected lift coefficient, ONERA M4R, M=0.492

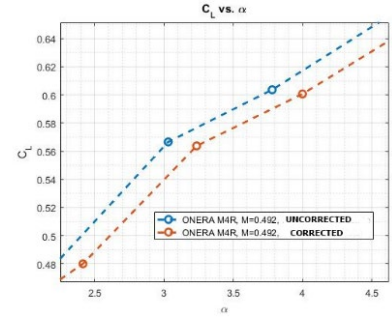

Fig. 5: Uncorrected lift coefficient vs. corrected lift coefficient, ONERA M4R, M=0.492, detail view

It can be seen that the magnitude of the corrections increases proportionally to the angle of attack. The increased values of the correction at high angles of attack confirm that the method is valid only for small disturbances, when the flow is characterized by only small deviations from the uniform flow.

At high angles of attack the accuracy of the results obtained using the potential flow model decreases significantly.

For the perforated walls, the corrections were computed following the procedure presented in the previous subsections and imposing the appropriate boundary conditions [11].

The experiments for the “Common Research Model - CRM” were carried out in the "sweep" mode, i.e. the angle of incidence was varied continuously, between the limits specified for each experiment in the test matrix, and having a movement speed of 3°/s.

During this movement, all channels of interest (time, incidence, pressures, temperature, balance signals, etc.) were read. Forces and moments were measured using the 2″ TASK balance .

The results were corrected for the effect of perforated walls using the previously described procedure and defining appropriate boundary conditions.

To verify the corrected results, they were compared with the results obtained for the NASA CRM model in the NTF (National Transonic Facility) and AMES wind tunnels.

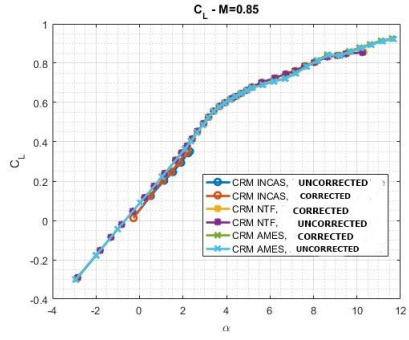

Fig. 6: Uncorrected lift coefficient, vs. corrected lift coefficient, CRM INCAS and NASA models, M=0.85

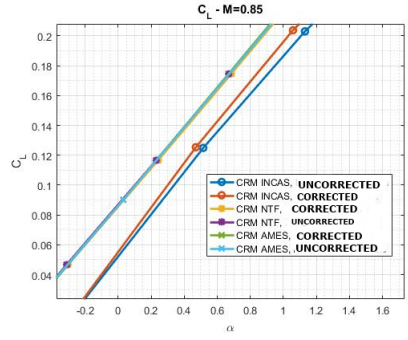

Fig. 7: Uncorrected lift coefficient, vs. corrected lift coefficient, CRM INCAS and NASA models, M=0.85, detail view

The difference between the uncorrected and the corrected lift coefficient in the case of the INCAS results has a greater magnitude than this difference in the case of the NASA wind tunnel results, but shows the same tendency towards a negative value with increasing incidence.

3. PERFORATED WALL CORRECTIONS USING MEASURED BOUNDARY CONDITIONS. THE ONE-VARIABLE METHOD

The assumption underlying the one-variable method is that the axial component of the interference velocity u_W satisfies the differential equation inside the experimental chamber, including the volume occupied by the model [3].

$$u_W = \frac{\partial \varphi_W}{\partial x} \tag{28}$$

$$\beta^2 \frac{\partial^2 u_W}{\partial x^2} + \frac{\partial^2 u_W}{\partial y^2} + \frac{\partial^2 u_W}{\partial z^2} = 0 \tag{29}$$

Thus:

$$u_W = u - u_M \tag{30}$$

The boundary conditions were obtained by measuring the pressure distributions on the walls of the test section [12].

The one-variable method used to determine the wall corrections in this paper consists of solving a Dirichlet-type problem. Thus, the flow field is represented by the double integral [13]:

$$u_W(r_0) = \iint_S f(r) \frac{\partial}{\partial n}\left(\frac{1}{4\pi|r_0 - r|}\right) dS \tag{31}$$

where f is the doublet intensity, S is the test section surface and $\frac{\partial}{\partial n}$ is the normal derivative.

When $r_0 \to r_k \in S$ and the observation point r_0 approaches r_k, the above equation becomes the Fredholm integral equation [14].

$$u_W(r_k) = -\frac{1}{2} f(r_k) + \iint_S f(r) \frac{\partial}{\partial n}\left(\frac{1}{4\pi|r_0 - r|}\right) dS \tag{32}$$

$u_W(r_k)$ it is assumed to be determined from pressure measurements.

$$u_W = u - u_M = -\beta\left(\frac{1}{2} Cp + \frac{\partial \varphi_M}{\partial x}\right) \tag{33}$$

If r_k is in the panel center, then results the following equation system [15]:

$$\sum_{j=1}^{N} A_{kj} f_j = u_k, \quad k = 1 \dots N \tag{34}$$

$$A_{kj} = \begin{cases} -\frac{1}{2}, & j = k \\ \iint_{S_j} \frac{\partial}{\partial n}\left(\frac{1}{4\pi|r_k - r|}\right) dS, & j \neq k \end{cases} \tag{35}$$

After computing the intensities, u_W can be determined for any r_0 [16].

$$\varepsilon(x, y, z) = \frac{1}{\beta} u_W(\tilde{x}, y, z) \tag{36}$$

$$\Delta\alpha_z(x, y, z) = \int_{\tilde{x}_R}^{\tilde{x}} \frac{\partial u_W}{\partial y}(\tilde{x}, y, z) d\tilde{x} - \frac{\partial \varphi_M}{\partial y}(\tilde{x}_R, y, z) \tag{37}$$

The results presented in this subsection were obtained for the ONERA M4R model, in the INCAS trisonic wind tunnel, 0.7 and 0.85 Mach numbers.

To verify the results, for Mach numbers 0.7 and 0.85, the lift and drag coefficients were compared with a series of results obtained for the ONERA M5 model in the JAXA trisonic wind tunnel [17].

Also, the data obtained in this chapter is compared with the results for the ONERA M4R model in the case of homogeneous boundary conditions, defined by means of the porosity parameter, P.

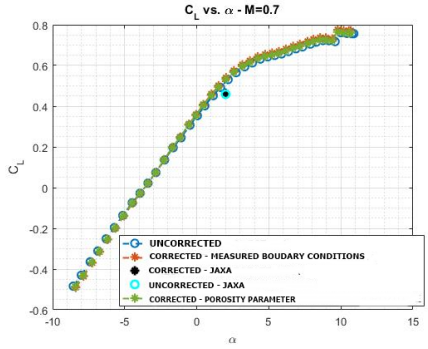

Fig. 8: Uncorrected lift coefficient vs. corrected lift coefficient by using measured and homogeneous boundary conditions, ONERA M4R and M5, M=0.7

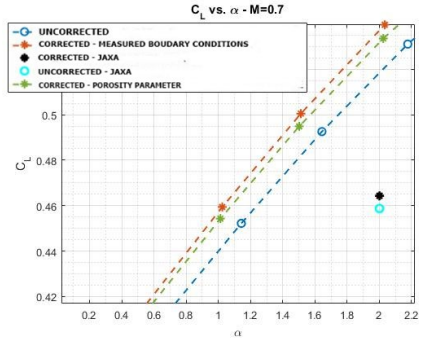

Fig. 9: Uncorrected lift coefficient vs. corrected lift coefficient by using measured and homogeneous boundary conditions, ONERA M4R and M5, M=0.7, detail view

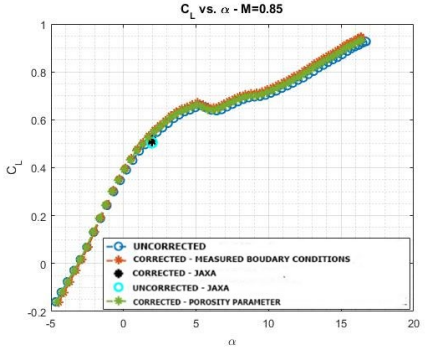

Fig. 10: Uncorrected lift coefficient vs. corrected lift coefficient by using measured and homogeneous boundary conditions, ONERA M4R and M5, M=0.85

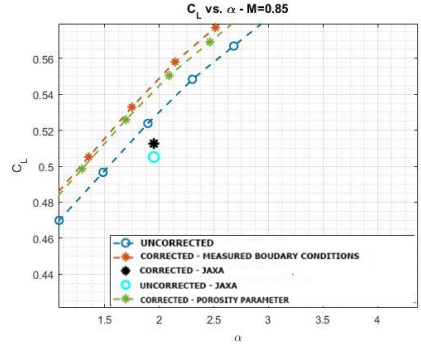

Fig. 11: Uncorrected lift coefficient vs. corrected lift coefficient by using measured and homogeneous boundary conditions, ONERA M4R and M5, M=0.85, detail view

For 0.7 and 0.85 Mach numbers, both the corrected and uncorrected results do not perfectly match the JAXA wind tunnel results for ONERA M5, but it can be seen that their trend after applying the correction is the same. For an incidence angle of approximately 2^0, the relative error between the corrected and uncorrected lift coefficient for ONERA M5 is 1.2% for M=0.7 and 1.46% for M=0.85. For ONERA M4R, at the same incidence angle, these relative error values are 1.5% for M=0.7 and 1.7% for M=0.85. The differences may occur due to the fact that there may be small geometrical differences between the two models, they were tested in two different wind tunnels and also the results obtained in this thesis do not take into account the interference due to the model support. Furthermore, the magnitude of corrections for ONERA M4R is larger than for ONERA M5 [9]. This may be due to the blockage generated by the two models in the two wind tunnels [18].

A software to automatically compute wall corrections for the INCAS trisonic wind tunnel has been developed. The software uses two types of boundary conditions, measured and homogeneous, defined by means of the porosity parameter.

For both situations, the input data are the geometric data of the model and wind tunnel, the uncorrected values for the measured parameters, the singularity distributions used in the model representation, as well as the boundary conditions.

The software initially determines the intensities of the singularities used in the representation of the model, then performs the calculation of the interference at any point in

the test section. After calculating the corrections, they are applied to the coefficients of forces and moments, as well as to the other parameters that need to be corrected.

4. CONCLUSIONS

The main purpose of this paper was to evaluate the interferences caused by the wind tunnel walls and the effect they have on the measured data. The data must also go through a correction process whose purpose is to eliminate the influence of the limited dimensions of the flow and bring them to a form independent of the characteristics of the wind tunnel.

The solid wall corrections for the ONERA M4R model were determined. As expected, after applying the corrections, both Mach number and dynamic pressure were characterized by higher values. At the same time, a slight increase in the magnitude of the correction could be observed with the increase of the angle of attack.

The increased values of the correction appearing at large incidence angles confirm that the method used is valid only for small disturbances, when the flow is characterized by only small deviations from the uniform flow. At high angles of attack the accuracy of the results obtained using the potential flow model decreases significantly.

In the case of perforated walls, correction calculations using homogeneous boundary conditions were performed following the presented procedure and imposing the appropriate boundary conditions. The magnitude of the corrections was found to be smaller than for solid walls due to the fact that one of the basic characteristics of perforated walls is the mechanical minimization of interference during experiments.

Perforated wall corrections were also determined for the CRM model, placed in the INCAS trisonic wind tunnel. To validate the corrected results, they were compared with the results obtained for the NASA CRM model in the NTF and AMES wind tunnels.

The interference due to the walls was also evaluated using a method that required the measurement of boundary conditions. The difference between the theoretical approach to the problem and the use of experimentally obtained boundary conditions consisted in replacing the idealized boundary condition with the measured one.

The one-variable method used involved solving a Dirichlet-type problem, which has a unique solution inside a region if the boundary conditions are specified at any point on that surface.

To verify the results obtained at Mach numbers 0.7 and 0.85, the lift and drag coefficients were compared with a series of results obtained for the ONERA M5 model in the JAXA trisonic wind tunnel.

The data were also compared with those also obtained for the ONERA M4R model for the case where the corrections were determined using homogeneous boundary conditions.

Both in the case of Mach number and dynamic pressure the corrected values led to their lower magnitudes. At the same time, the corrections determined using boundary conditions defined by means of the porosity parameter are smaller than those determined using measured boundary conditions. This may suggest that the porosity parameter was underestimated but, at the same time, the difference may also be caused by the homogeneity of the boundary condition, which defines identical phenomena in any region of the wall, regardless of the position of the model.

ACKNOWLEDGEMENT

This paper is a summary of the PhD thesis "Contributions to the Study of Wind Tunnel Wall Corrections", which was awarded the *"Nicolae Tipei" Prize, PhD thesis section*, and was presented at the *40th edition of the "Caius Iacob" Conference on Fluid Mechanics and its Technical Applications*, held in Bucharest, Romania, on October 19–20, 2023.

REFERENCES

[1] E. Toledano, *Improvement of Subsonic Wall Corrections in an Industrial Wind Tunnel*, Montreal, 2019.
[2] J. D. Keller, *Numerical Calculation of Boundary-Induced Interference in Slotted or Perforated Wind Tunnels Including Viscous Effects in Slots*, Langley Research Center, Hampton, 1972.
[3] P. Ashill, J. Hackett, M. Mokry and F. Steinle, Boundary Measurements Methods, in *Wind Tunnel Wall Corrections*, AGARD, 1998.
[4] E. L. Walker, *Statistical Calibration and Validation of a Homogeneous Ventilated Wall-Interference Correction Method for the National Transonic Facility*, Virginia Polytechnic Institute and State University, Virginia, 2005.
[5] B. F. R. Ewald, *Wind Tunnel Wall Correction*, AGARD, 1998.
[6] M. Mokry and R. Galway, *Analysis of Wall Interference Effects on ONERA Calibration Models in the NAE 5-ft. Wind Tunnel*, NRC Aeronautical Report, Ottawa, 1977
[7] C. Lo and R. Oliver, *Boundary* Interference in a Rectangular Wind Tunnel with Perforated Walls, AEDC, 1970
[8] J. D. Anderson, Modern Compressible Flow, 1990.
[9] M. Manea (Burghiu), C. I. Stoica and A. Burghiu, Wind Tunnel Perforated Wall Corrections for the ONERA M4R Model, *U.P.B. Scientific Bulletin,* vol. **84**, no. 4, pp. 17-28, 2022.
[10] M. Manea, A. Burghiu, Lift Interference in Wind Tunnels with Perforated and Solid Walls, *INCAS Bulletin,* vol. **13**, no. 1/2021, 2021, https://doi.org/10.13111/2066-8201.2021.13.1.11
[11] N. Ulbrich, *Description of Panel Method Code ANTARES*, Ames Research Center, California, 2000.
[12] M. Burghiu (Manea) and A. Burghiu, Evaluation of the Porosity Parameter for a Perforated Wall Wind Tunnel Using Measured Wall Pressure Distributions," *INCAS Bulletin,* vol. **14**, no. 3, pp. 3-9, 2022, https://doi.org/10.13111/2066-8201.2022.14.3.1
[13] M. Mokry, *Subsonic Wall Corrections in the IAR 1.5m Wind Tunnel*, Institute for Aerospace Research, Ottawa, 2006
[14] M. Mokry and J. P. R. Digney, Doublet-Panel Method for Half-Model Wind-Tunnel Corrections, *Journal of Aircraft,* 1987.
[15] A. Toledano, C. Broughton, F. Morency and J. Weiss, Improvement of Subsonic Wall Corrections in an Industrial Wind Tunnel, in *CASI*, Montreal, 2015.
[16] A. Toledano, F. Morency and J. Weiss, Improvement of Wall Corrections at the National Research Council's Trisonic Wind Tunnel, *Journal of Aircraft,* vol. **56**, no. 6, 2019.
[17] A. Hashimoto and M. Kohzai, Wall Interference Analysis by Whole Wind Tunnel CFD, in *5th Symposium on Integrating CFD and Experiments in Aerodynamics*, Tokyo, 2012.
[18] F. Steinle and E. Stanewsky, *Wind Tunnel Flow Quality and Data Accuracy Requirements*, AGARD, 1982.